crystals

MDPI

Article

Synthesis and High-Pressure Stability Study of Energetic Molecular Perovskite DAI-X1

Tingting Yan *, Han Li, Dongyang Xi, Linan Liu, Lei Sun and Dinghan Jin

School of Materials Science and Engineering, Shenyang Jianzhu University, Shenyang 110168, China; lhan111@stu.sjzu.edu.cn (H.L.); xidy12@sjzu.edu.cn (D.X.); liu12063236@stu.sjzu.edu.cn (L.L.); sl24@stu.sjzu.edu.cn (L.S.); jdh0220@stu.sjzu.edu.cn (D.J.)
* Correspondence: yantt@sjzu.edu.cn

Abstract: In the pursuit of advancing the knowledge of energetic materials, we successfully formulated the energetic perovskite DAI-X1 with the chemical formula ($C_{12}H_{50}I_6N_3Na_2O_{36}$). Energetic perovskites hold great promise in various applications, including high-energy storage and propulsion systems, due to their unique combination of high energy density and structural versatility. DAI-X1, in particular, has attracted our attention because of its potential for optimized performance in these areas. We conducted an in-depth investigation into the high-pressure stability of DAI-X1 using in situ high-pressure Raman spectroscopy analysis. DAI-X1 possesses a cubic ABX_3 perovskite structure, and notable modifications in its Raman spectroscopic characteristics were noted within the pressure interval of 2.5–7.8 GPa, indicating structural instability under high pressure and suggesting a possible phase transition. Upon pressure release following compression to 12.5 GPa, the Raman spectra exhibit partial reversibility of the phase transition, as certain characteristic peaks return to their original positions while others retain irreversible shifts. This study establishes fundamental understanding for investigating high-pressure responses in DAI-X1 and analogous energetic materials.

Keywords: high pressure; phase transition; molecular perovskite; partially reversible; energetic materials

check for updates

Academic Editor: Maria Gazda

Received: 15 May 2025
Revised: 28 May 2025
Accepted: 29 May 2025
Published: 1 June 2025

Citation: Yan, T.; Li, H.; Xi, D.; Liu, L.; Sun, L.; Jin, D. Synthesis and High-Pressure Stability Study of Energetic Molecular Perovskite DAI-X1. *Crystals* **2025**, *15*, 530. https://doi.org/10.3390/cryst15060530

Copyright: © 2025 by the authors. Licensee MDPI, Basel, Switzerland. This article is an open access article distributed under the terms and conditions of the Creative Commons Attribution (CC BY) license (https://creativecommons.org/licenses/by/4.0/).

1. Introduction

Energetic materials [1–4], as strategic national resources, are of paramount significance in both modern defense and civilian applications. In the military domain, they serve as the lifeblood of advanced weaponry. Military propellants are carefully engineered to provide the high-energy thrust required for missiles, rockets, and artillery shells, enabling them to reach their intended targets with precision and power. Explosives, on the other hand, are used in a variety of military operations, such as mine-laying, demolition of enemy infrastructure, and as warheads in various munitions. In aerospace pyrotechnics, energetic materials play a crucial role in ensuring the successful ignition and operation of spacecraft systems.

In the civilian sector, energetic materials are equally indispensable. The performance of energetic materials has a direct and far-reaching impact on national security and economic development [5–8]. The continuous advancement of high-tech weapon systems has set extremely stringent requirements for energetic materials, demanding that they achieve "high energy output, low sensitivity, and environmental compatibility" [9–11].

However, conventional nitroamine-based compounds (e.g., RDX, HMX) are approaching their theoretical energy density ceilings. The energy density of these materials, which is

a measure of the amount of energy stored per unit mass, has reached a limit due to their chemical structure. Moreover, they suffer from high mechanical sensitivity, which means they can be easily detonated by external mechanical impacts such as shock, friction, or impact. This is a significant safety concern, as it increases the risk of accidental explosions during manufacturing, storage, and transportation. Their poor thermal stability also poses a considerable challenge. At relatively high temperatures, these materials may decompose or even explode, which not only reduces their effectiveness but also poses a serious threat to the surrounding environment and personnel [12,13]. These limitations have severely restricted the development of next-generation energetic systems [14].

To overcome the performance limitations of conventional energetic materials, researchers have turned to molecular perovskites with tailorable properties [15–18]. These materials feature an ABX_3-type crystalline architecture, where the A-site is occupied by organic amine cations (e.g., dabco), the B-site by metal ions (e.g., K^+), and the X-site by energetic anions (e.g., ClO_4^-) [19–21]. The modular assembly strategy enables precise tuning of both energy output and stability. Studies reveal that such materials not only exhibit outstanding detonation performance (with velocities reaching 9.5 km/s) but also demonstrate unique environmental responsiveness [22]. Notably, their organic–inorganic hybrid structure allows controllable phase transitions under external stimuli (e.g., pressure, temperature), offering a novel paradigm for developing next-generation smart energetic materials [23].

In 2018, the first report of $(H_2dabco)M(ClO_4)_3$ molecular perovskite energetic crystals (dabco = 1,4-diazabicyclo[2.2.2]octane; M = $Na^+/K^+/Rb^+/NH_4^+$ denoting DAP-1/2/3/4) [24–26] marked a significant milestone. The straightforward solution-phase self-assembly of oxidizers and reducers into perovskite frameworks confers these molecular perovskite energetic crystals with unique benefits. The solution-phase self-assembly process is relatively simple and cost-effective compared to traditional high-temperature and high-pressure synthesis methods. It also allows for precise control over the composition of the materials, enabling researchers to tune the properties of the molecular perovskite energetic crystals to meet specific requirements. This compositional tunability and scalability in production have driven growing scientific interest [27,28].

In 2023, a team led by Zhi Hong Yu made significant advancements in the field of material science. The iodine-rich molecular perovskite $(H_2dabco)[Na(H_4IO_6)_3]$ (DAI-X1), based on the tetrahydroxyiodate anion ($H_4IO_6^-$), was reported as a novel energetic bactericide, which prompted our investigation into its high-pressure behavior and properties [18,29]. The inclusion of the iodine-rich tetrahydroxyiodate anion in the molecular perovskite structure may endow DAI-X1 with unique properties, such as enhanced energy output and antibacterial activity.

DAI-X1 is considered to be a suitable energetic material due to its unique chemical structure and composition. The presence of high-energy chemical bonds contributes to its high energy density. These bonds can undergo exothermic decomposition reactions, releasing a large amount of energy when triggered. In addition, its structural design allows effective energy release and propagation, which is the basic characteristic of energetic materials. DAI-X1 has an iodine-containing portion and a nitrogen-rich portion. These groups contribute to high energy density due to their strong chemical bonds and the possibility of exothermic decomposition reactions. For example, the iodine-carbon bond in the molecule can release a lot of energy when it breaks, and the nitrogen–nitrogen bond in the amine structure can also participate in the high-energy decomposition process.

According to the calculation, the formation enthalpy of DAI-X1 is approximately −1883.11 kJ/mol. The negative value indicates that the formation of DAI-X1 by its constituent elements is an exothermic process, which is beneficial to energetic materials. The

large negative enthalpy of formation indicates that DAI-X1 can release a large amount of energy during the decomposition process, making it a potential candidate for high-energy applications. It exhibits a heat of explosion of 2479.09 kJ/mol. According to the density (ρ = 2.84 g/cm^3) and formation enthalpy of DAI-X1, the detonation heat (Q^d) of DAI-X1 was estimated to be 2.74 kJ/g. Additionally, its detonation velocity (D^d) reaches 7.07 km/s. In addition, high-energy electrical discharges can also be used to initiate the detonation of DAI-X1. By applying a high-voltage electrical pulse to a small amount of a sensitive explosive material in close proximity to DAI-X1, a shock wave can be generated, which can then initiate the detonation of DAI-X1.

DAI-X1 has the potential to act as an oxidizer in energetic formulations. The chemical structure of DAI-X1 contains oxygen-rich functional groups, which can provide the necessary oxygen for the combustion or decomposition of fuels. For the perovskite framework, it is reasonable to configure the unit-valence period anion on site X, because it has both the strong oxidizing ability to achieve the required high ignition performance and the acceptable sensitivity to achieve reliable ignition. Studies have confirmed that ion-based energy substances exhibit strong oxidation, high sensitivity and rapid exothermic behavior of iodine. Iodine exhibits a bactericidal effect and as a decomposition product, it exhibits a biofriendly effect, thus showing a huge green main explosive.

Pressure [30,31], as a fundamental thermodynamic parameter of material states, can directly modify atomic spacing and electronic structure without chemical doping. As an extreme condition, high pressure has been widely applied in studies of superconducting materials, energetic materials [32,33], and perovskites [34]. In the realm of energetic materials, high-pressure research holds dual significance. Energetic materials, such as propellants, explosives, and pyrotechnics, are designed to release large amounts of energy in a controlled manner. Understanding their behavior under high-pressure conditions is crucial for ensuring their safe and effective use. High-pressure studies can reveal how these materials respond to extreme forces, such as those encountered during storage, transportation, or detonation. This knowledge can be used to develop safer handling procedures and to optimize the performance of energetic materials in various applications [35].

Under high pressure, the atomic spacing in molecular perovskite energetic materials can be significantly reduced, leading to changes in the electronic structure and chemical bonding. This can result in enhanced energy output, as more energy can be stored in the compressed material. Under high-pressure conditions, these interactions can be significantly altered, leading to changes in the material's structure and behavior. Understanding these interactions and their impact on the material's properties is essential for developing a comprehensive understanding of the high-pressure response of molecular perovskite energetic materials. High pressure can also modify the sensitivity of the materials, potentially reducing their mechanical sensitivity and improving their safety. Recent advancements in high-pressure techniques, particularly diamond anvil cell technology, have led to significant progress in studying pressure-induced phase transitions of conventional energetic materials. However, the high-pressure response of molecular perovskite energetic materials is a research frontier that has not yet been fully elucidated. In particular, the relationship between pressure-driven structural changes and energy release mechanisms remains poorly understood.

On this basis, the energetic molecule perovskite DAI-X1 ($C_{12}H_{50}I_6N_3Na_2O_{36}$) was synthesized in this study, and its structure and vibration properties under high pressure were systematically studied. The purity of the synthesized samples was confirmed by X-ray diffraction (XRD), and infrared (IR) spectroscopy revealed key vibration modes, including N–H and C–H stretching modes. In order to explore its high-pressure stability, an in situ high-pressure Raman spectroscopy test of up to 12.5 GPa was performed using a diamond

anvil. Raman spectra show obvious changes between 2.5 and 7.8 GPa, indicating that the structure is unstable and there may be pressure-induced phase transition.

Remarkably, upon decompression from 12.5 GPa, the Raman spectra partially reverted to their initial state, indicating partial reversibility of the structural transformation. These findings demonstrate that DAI-X1 undergoes a phase transition under pressure, which has critical implications for its behavior in extreme environments. This work not only advances the fundamental understanding of molecular perovskite energetic materials but also provides valuable insights for designing next-generation high-energy-density materials with improved stability and safety.

2. Experimental Section

2.1. Experimental Material

Reagents were sourced as follows: periodic acid (H_5IO_6, 99%), sodium periodate ($NaIO_4$, 99%), and anhydrous ethanol from Shanghai Aladdin Biochemical Technology (Shanghai, China); triethylenediamine (dabco, 98%) from Sinopharm Chemical Reagent (Shanghai, China). All of these reagents were used without further purification, as the specified purities were considered sufficient for the synthesis and characterization procedures in this study.

2.2. Sample Preparation

DAI-X1 was prepared according to the literature methods [36]. In a typical synthesis procedure, sodium periodate (1 mmol) and dabco (0.7 mmol) were first dissolved in deionized water (4 mL). Deionized water was used to ensure the absence of any ionic impurities that could interfere with the reaction. The solution was stirred continuously to ensure complete dissolution of the reagents, resulting in a clear solution. The clear appearance of the solution indicates that the reagents had fully dissolved and were evenly distributed in the water.

Then, an aqueous periodic acid solution (3 mmol in 5 mL H_2O) was slowly added to the above-mentioned clear solution. The slow addition was crucial to control the reaction rate and allow for the proper formation of the DAI-X1 compound. As the periodic acid solution was added, a precipitation reaction occurred, and the DAI-X1 precipitate began to form.

After the precipitation was complete, the precipitated DAI-X1 was filtered using a fine-pore filter paper to separate it from the reaction solution. The obtained precipitate was then washed three times with anhydrous ethanol. The washing process was essential to remove any unreacted reagents or by-products that might be present on the surface of the precipitate.

2.3. Experimental Characterization

Phase identification of the synthesized sample was performed under ambient conditions using powder X-ray diffraction (XRD-7000, Shimadzu, Kyoto, Japan) with Cu Kα1 radiation (λ = 1.5406 Å). The diffraction patterns were collected in the 2θ range of 10° to 60°. This range was chosen because it typically contains the characteristic diffraction peaks for most crystalline materials, allowing for a comprehensive analysis of the phase composition of the synthesized DAI-X1. The scanning speed was 1°/min. A slow scan rate helps to improve the resolution of the diffraction peaks, enabling more accurate identification of the phases present in the sample. The instrument works under the condition of 40 kV and 200 mA, which provides sufficient X-ray intensity for accurately collecting diffraction peaks. Rietveld refinement of the XRD patterns was subsequently conducted using the GSAS-II EXPGUI software package. Rietveld refinement of XRD patterns was then performed using

the GSAS-II software package. Rietveld refinement is a method to refine the crystal structure parameters of materials based on the measured XRD data [37–39]. By comparing the experimental XRD data with the theoretical diffraction patterns calculated by the refined crystal structure model, the goodness of fit can be evaluated, and any difference can be used to further optimize the crystal structure parameters.

The Fourier transform infrared spectrometer (FTIR) is a Nicoleti S5 infrared spectrometer produced by the Nicholas company in the United States. It is a precise and high-precision analytical instrument. The wide wavenumber range is 4000–350 cm^{-1}. The structure and chemical bond of the molecule are studied, and the chemical structure of the molecule is speculated.

2.4. High Pressure Experiment of DAI-X1

In situ high-pressure experiments were conducted using a symmetric diamond anvil cell (DAC, Shanghai Ouluodia Superhard Materials Technology Co., Ltd., Shanghai, China) with 400 μm culet diameters. A T301 stainless steel gasket was pre-indented to 40–50 μm thickness, followed by laser-drilling a 130 μm diameter sample chamber at the center. The DAI-X1 sample was loaded into the chamber together with 1–2 ruby spheres for pressure calibration via the R1 fluorescence line shift method [40]. Throughout the experiments, the ruby fluorescence lines remained sharp and well-resolved even at maximum pressure [41]. All measurements were performed under ambient temperature conditions.

High-pressure Raman spectra were recorded in situ using a HORIBA XPLORA PLUS spectrometer (638 nm diode laser excitation) connected to a Pylon 100B CCD detector with liquid nitrogen cooling (HORIBA, Kyoto, Japan). The liquid nitrogen cooling helps to reduce the thermal noise in the detector, improving the sensitivity and signal-to-noise ratio of the Raman spectra. The experiments were performed using a spectral resolution of 1 cm^{-1} and an approximately 3 μm diameter focal spot. To avoid sample damage, the laser power should be kept at a steady 10 mW.

3. Results and Discussion

The final results of Rietveld refinement of DAI-X1 are shown in Figure 1. A strikingly high correlation is observed between the observed experimental data points and the calculated data curve. Each peak in the experimental pattern is accurately reproduced by the calculated pattern, indicating a close match in both peak positions and intensities. This high-fidelity agreement between the observed and calculated data not only validates the accuracy of the refinement process but also serves as compelling evidence for the high purity of the synthesized DAI-X1 sample. The refinement reliability was verified by the following parameters: Rwp = 7.88%, Rp = 6.15%, and χ^2 = 1.54.

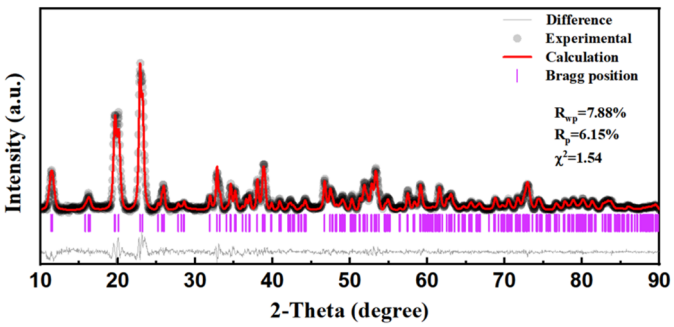


Figure 1. Rietveld refinement of DAI-X1 XRD pattern showing experimental data (gray circles), calculated data (red line), difference plot (gray line, bottom), and purple vertical ticks (|) marking bragg reflection positions.

The infrared spectrum of DAI-X1 is shown in Figure 2. One of the prominent absorption bands observed in the IR spectrum of DAI-X1 is located at 3023 cm^{-1}. This absorption band can be confidently attributed to the C–H stretching vibration. In organic molecules, C–H bonds are ubiquitous. Another absorption band is located at 3498 cm^{-1}. This band can be ascribed to the N–H stretching vibration. Nitrogen–hydrogen bonds are also important functional groups in many energetic materials, including DAI-X1. The N–H bond is polar due to the difference in electronegativity between nitrogen and hydrogen atoms. As a result, it has a characteristic stretching vibration frequency in the IR spectrum.

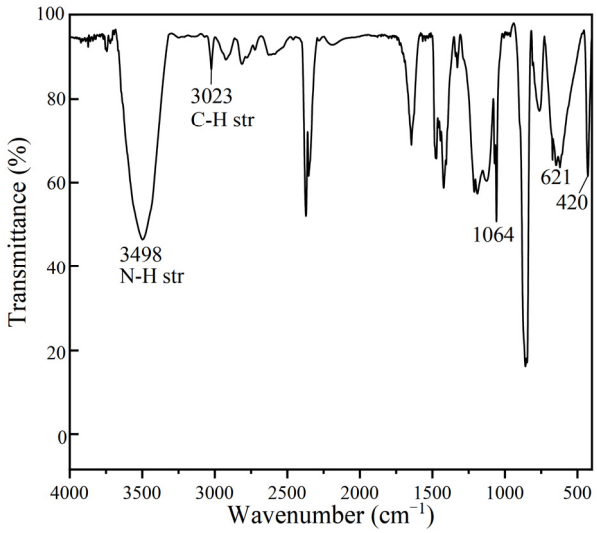


Figure 2. FTIR spectrum of DAI-X1. The key absorption bands were marked as follows: 3023 cm^{-1} (C–H stretching vibration) and 3498 cm^{-1} (N–H stretching vibration).

The absorption peak observed at 420 cm^{-1} in the infrared (IR) spectrum is attributed to C–C bending vibrations, specifically low-frequency skeletal deformations within the molecular framework. This region of the IR spectrum (below~600 cm^{-1}) is dominated by heavy-atom motions, out-of-plane bending, and torsional vibrations of carbon–carbon bonds, particularly in rigid or cyclic structures. The absorption peak at approximately 620 cm^{-1} is often attributed to the N–H bending vibration. In organic compounds, nitrogen–hydrogen bonds can undergo various types of bending motions. The absorption at 1064 cm^{-1} is assigned to the C–C stretching vibration. It may also be associated with the in-plane bending or ring-breathing vibrations of a cyclic structure, especially if it is part of a conjugated system. For example, in some cyclic ethers or lactones, C–C stretching vibrations can occur in this region.

These features are essential for understanding the chemical behavior and energetic properties of DAI-X1, and they serve as a starting point for further detailed structural analysis and functional studies.

DAI-X1 crystallizes in the monoclinic system with the C_2/m space group. The unit cell parameters are as follows: a = 11.2264 Å, b = 10.8733 Å, c = 7.7133 Å, $\alpha = \gamma = 90.000°$, $\beta = 90.064°$, and V = 941.5 $Å^3$ [36]. The ABX_3 type perovskite structure of DAI-X1 is shown in Figure 3, where $H_2dabco_2^+$ acts as the A-site cation, Na^+ serves as the B-site cation, and $H_4IO_6^-$ bridges as the X-site anion. Each Na^+ ion is coordinated by six oxygen atoms derived from six $H_4IO_6^-$ anions, while each $H_4IO_6^-$ anion bridges two Na^+ ions, forming a three-dimensional anionic framework. Compared to the smaller IO_4^- anion, the larger $H_4IO_6^-$ anion induces structural distortion in the anionic framework of DAI-X1 due to its bulkier size.

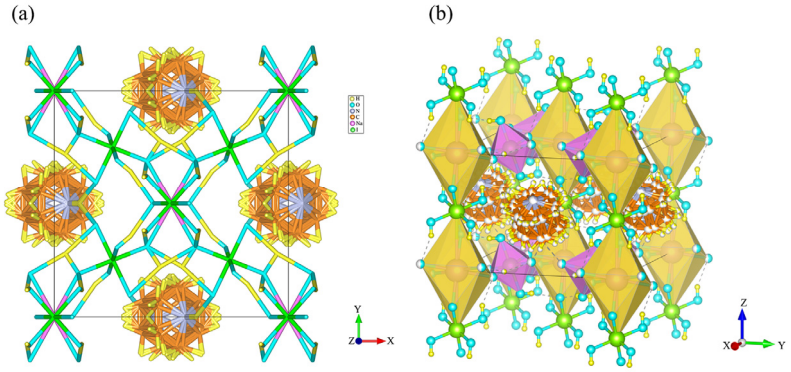


Figure 3. (**a**) **Stick and** (**b**) **polyhedral structures** of DAI-X1. Color code: H (red), O (blue), N (light purple), C (orange), Na (pink), I (green).

High-pressure studies of DAI-X1 are of utmost importance as they provide a unique opportunity to explore the structural and energetic responses of the material under extreme conditions. The conformational responses of energetic materials under such conditions are not well-understood, and high-pressure studies directly address this important research gap in this material class. When subjected to high pressure, the atoms and ions within the DAI-X1 crystal lattice are forced closer together, which can lead to changes in the crystal structure. These changes can, in turn, affect the energy storage capacity, the sensitivity to external stimuli, and the overall stability of the material. By conducting high-pressure experiments on DAI-X1, researchers can gain valuable insights into the fundamental mechanisms governing the behavior of energetic materials.

We conducted an in-depth high-pressure study using Raman spectroscopy, covering a pressure range from 0 to 12.5 GPa. Figure 4 displays pressure dependent spectra (80–3400 cm^{-1}), where lattice region vibrations reveal collective molecular dynamics and intermolecular coupling, providing clear phase transition signatures.

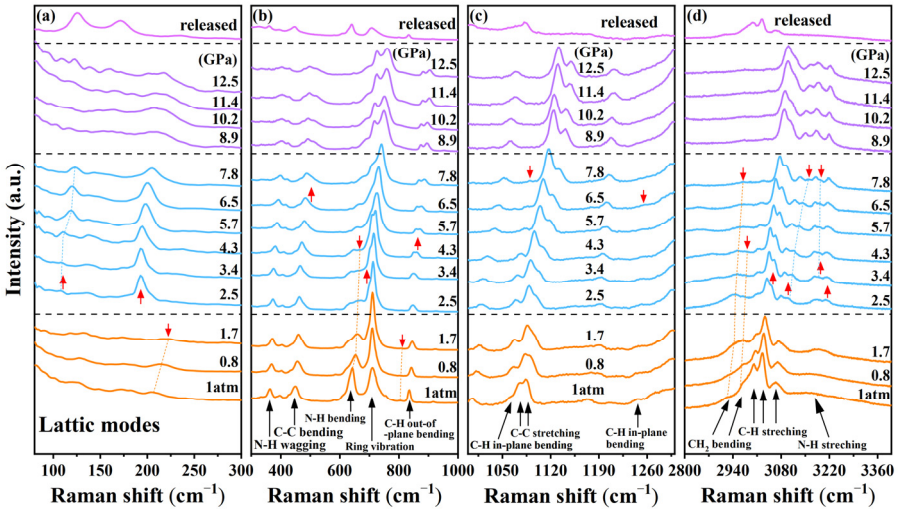


Figure 4. Raman spectra of DAI-X1 at high pressure (**a**) 80–300 cm^{-1}, (**b**) 300–1000 cm^{-1}, (**c**) 1000–1300 cm^{-1}, and (**d**) 2800–3400 cm^{-1}. The black numbers on each curve represent the corresponding pressure value (unit: GPa). The orange lines represent ambient phase I, the blue lines represent phase transition interval, and the purple lines represent high pressure phase II. The top light purple line represents the Raman spectrum after pressure relief.

As we gradually increased the pressure on the DAI-X1 sample, a series of remarkable changes unfolded in the Raman spectra. At relatively low pressures, specifically when

the pressure reached 1.7 GPa, two Raman vibrational peaks at 207 cm^{-1} and 804 cm^{-1} disappeared, as clearly indicated by the downward arrows in Figure 4.

When the pressure was further increased to 2.5 GPa, as shown in Figure 4a, new vibrational peaks suddenly emerged in the lattice region at 108 cm^{-1} and 196 cm^{-1}. Simultaneously, as seen in Figure 4b, d, new peaks appeared at 695 cm^{-1}, 3053 cm^{-1}, 3102 cm^{-1}, and 3215 cm^{-1}, as marked by the upward arrows. These peaks are likely associated with the vibrational modes of the functional groups within the DAI-X1 molecule, which are also affected by the high-pressure environment. The simultaneous appearance of these new peaks in different frequency regions provides strong evidence that the crystal begins to transition from ambient-pressure Phase I to high-pressure Phase II.

As the pressure continued to rise to 3.4 GPa, a novel peak emerged in the vicinity of the N–H stretching vibration area (3188 cm^{-1}). The appearance of this new peak suggests that the high-pressure environment is causing changes in the hydrogen-bonding network within the DAI-X1 crystal. However, as the pressure was further increased to 7.8 GPa, this peak vanished. At a pressure of 4.3 GPa, the Raman scattering signals observed at 831 cm^{-1} and 1396 cm^{-1} were entirely obscured by the scattering background. Concurrently, as the initial Raman peaks vanished, a novel vibrational peak appeared at 862 cm^{-1}, as depicted by the upward arrow. As the pressure steadily rose to 7.8 GPa, all Raman vibrational peaks indicated by downward arrows vanished, indicating the end of the phase change.

When the pressure continues to increase from 7.8 GPa to 12.5 GPa, the observed Raman peaks remain essentially consistent and continuously change only slightly. Upon pressure release, the Raman spectrum largely reverted to its original state, though with minor irreversible changes in certain modes (Figure 4d), indicating partial reversibility of the phase transition. This behavior suggests that while the high-pressure-induced structural changes in DAI-X1 are predominantly reversible, some localized alterations (e.g., bond distortions or residual strain) may persist.

Figure 5 presents the pressure dependent variation curves of Raman vibrational modes in DAI-X1. Raman spectroscopy can be used to study the molecular vibration and lattice dynamics of materials. By analyzing the changes in the Raman peaks, we can gain insights into how the internal structure of DAI-X1 responds to the application of external pressure.

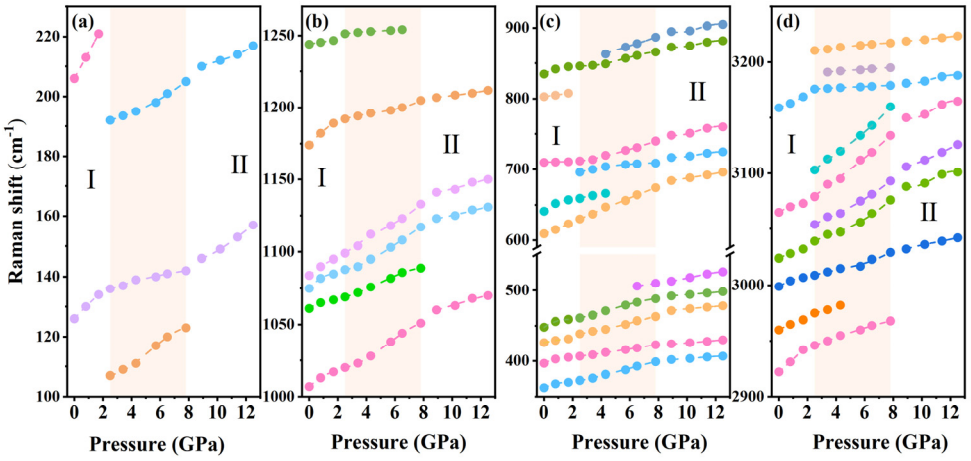


Figure 5. Raman vibration modes of DAI-X1 in the range of (**a**) 100–230 cm^{-1}, (**b**) 1000–1270 cm^{-1}, (**c**) 350–930 cm^{-1}, and (**d**) 2900–3250 cm^{-1} versus pressure. For clarity, linear fitting was performed. The light orange regions represent the phase boundaries between different phases.

As illustrated in Figure 5, the peak position shift curve displays a distinct discontinuity within the pressure range of 2.5–7.8 GPa. The observation of this discontinuity is consistent with the obvious phase transition interval identified in Raman spectroscopy. When a phase

transition occurs, the vibrational modes of the material's molecules are affected. The bonds between atoms may be stretched, compressed, or re-arranged, leading to changes in the energy levels of the vibrational states. These changes are manifested as shifts in the Raman peaks. The presence of a discontinuity in the peak position shift curve provides strong evidence that DAI-X1 undergoes a phase transition within the specified pressure range.

Upon the completion of the phase transition, it was observed that all vibrational modes displayed a blue shift [42]. The blue shift is when the pressure is applied, the atoms are forced to bond more closely together, resulting in stronger interaction. The blue-shift phenomenon continues as the pressure is increased until it reaches the peak experimental pressure of 12.5 GPa. At this point, the vibrational modes have reached their highest pressure under the experimental conditions. Based on the comprehensive experimental investigation, we propose that DAI-X1 might experience a structural phase transformation under elevated pressure.

Understanding the structural phase transformation of DAI-X1 under pressure is of great significance. It not only deepens our understanding of the fundamental properties of this material but also has potential implications for its applications. For example, in the development of high-performance energetic materials, the ability to control and tune the structural phase through pressure could lead to the design of materials with enhanced energy output, improved stability, and tailored sensitivity. This research provides a foundation for further exploration of the pressure-induced properties of DAI-X1 and may open up new avenues for the development of advanced materials for various high-tech applications.

4. Conclusions

In this comprehensive study, we delved deeply into the crystallographic properties of DAI-X1 under high-pressure conditions. Our approach was multi-faceted, combining the synthesized DAI-X1 crystals with the application of advanced experimental techniques, namely X-ray diffraction (XRD), diamond anvil cell (DAC) techniques, and in situ high-pressure Raman scattering. Each of these techniques played a crucial role in uncovering the mysteries of DAI-X1's behavior under extreme pressure. We observed the sudden appearance of new vibrational modes at 2.5 GPa. These new vibrational modes were not present in the Raman spectrum of DAI-X1 at lower pressures. Concurrently, we noticed significant discontinuities in the peak positions throughout the 2.5–7.8 GPa interval. These discontinuities are indicators of a high-pressure phase transition in DAI-X1. A phase transition occurs when a material changes from one crystalline structure to another in response to changes in external conditions such as pressure or temperature. Upon pressure release, the Raman spectra show partial recovery to their initial state.

These findings provide a basic framework for understanding the pressure-induced phase transition in such materials. By combining the data from XRD, DAC, and in situ high-pressure Raman scattering, we were able to gain a comprehensive understanding of the crystallographic properties of DAI-X1 under high pressure. The in-depth investigation of DAI-X1's high-pressure characteristics will have far-reaching implications. It will greatly facilitate the progress of research in the field of energetic molecular perovskite materials. Understanding the pressure-induced phase transition in DAI-X1 can help us design and develop new energetic materials with improved stability, energy output, and safety.

Author Contributions: Conceptualization, T.Y. and H.L.; methodology, D.X.; software, L.L.; formal analysis, L.S.; investigation, D.J.; writing—original draft preparation, H.L.; writing—review and editing, T.Y. and D.X.; funding acquisition, T.Y. All authors have read and agreed to the published version of the manuscript.

Funding: This research was funded by National Natural Science Foundation of China (Grant No. 11604224), and Foundation of Liaoning Province Education Administration (Grant No. LJ212410153027).

Data Availability Statement: The original contributions presented in this study are included in the article. Further inquiries can be directed to the corresponding author.

Conflicts of Interest: The authors declare no conflicts of interest.

References

1. Gao, H.; Zhang, Q.; Jean'ne, M.S. Fused heterocycle-based energetic materials (2012–2019). *J. Mater. Chem. A* **2020**, *8*, 4193–4216. [CrossRef]
2. Shang, Y.; Huang, R.-K.; Chen, S.-L.; He, C.-T.; Yu, Z.-H.; Ye, Z.-M.; Zhang, W.-X.; Chen, X.-M. Metal-free molecular perovskite high-energetic materials. *Cryst. Growth Des.* **2020**, *20*, 1891–1897. [CrossRef]
3. Zlotin, S.G.; Churakov, A.M.; Egorov, M.P.; Fershtat, L.L.; Klenov, M.S.; Kuchurov, I.V.; Makhova, N.N.; Smirnov, G.A.; Tomilov, Y.V.; Tartakovsky, V.A. Advanced energetic materials: Novel strategies and versatile applications. *Mendeleev Commun.* **2021**, *31*, 731–749. [CrossRef]
4. Muravyev, N.V.; Wozniak, D.R.; Piercey, D.G. Progress and performance of energetic materials: Open dataset, tool, and implications for synthesis. *J. Mater. Chem. A* **2022**, *10*, 11054–11073. [CrossRef]
5. Pang, W.-Q.; Yetter, R.A.; DeLuca, L.T.; Zarko, V.; Gany, A.; Zhang, X.-H. Boron-based composite energetic materials (B-CEMs): Preparation, combustion and applications. *Prog. Energy Combust. Sci.* **2022**, *93*, 101038. [CrossRef]
6. Yu, Q.; Yin, P.; Zhang, J.; He, C.; Imler, G.H.; Parrish, D.A.; Shreeve, J.n.M. Pushing the limits of oxygen balance in 1,3,4-oxadiazoles. *J. Am. Chem. Soc.* **2017**, *139*, 8816–8819. [CrossRef]
7. Anniyappan, M.; Talawar, M.B.; Sinha, R.K.; Murthy, K.P. Review on advanced energetic materials for insensitive munition formulations. *Combust. Explos. Shock Waves* **2020**, *56*, 495–519. [CrossRef]
8. Banik, S.; Yadav, A.K.; Kumar, P.; Ghule, V.D.; Dharavath, S. Unfolding the chemistry of FOX-7: Unique energetic material and precursor with numerous possibilities. *Chem. Eng. J.* **2022**, *431*, 133378. [CrossRef]
9. Herweyer, D.; Brusso, J.L.; Murugesu, M. Modern trends in "Green" primary energetic materials. *New J. Chem.* **2021**, *45*, 10150–10159. [CrossRef]
10. Bu, R.; Xiong, Y.; Zhang, C. π–π stacking contributing to the low or reduced impact sensitivity of energetic materials. *Cryst. Growth Des.* **2020**, *20*, 2824–2841. [CrossRef]
11. Li, G.; Zhang, C. Review of the molecular and crystal correlations on sensitivities of energetic materials. *J. Hazard. Mater.* **2020**, *398*, 122910. [CrossRef] [PubMed]
12. Liang, T.; Zhang, Y.; Ma, Z.; Guo, M.; Xiao, Z.; Zhang, J.; Dong, M.; Fan, J.; Guo, Z.; Liu, C. Energy characteristics and mechanical properties of cyclotrimethylenetrinitramine (RDX)-based insensitive high-energy propellant. *J. Mater. Res. Technol.* **2020**, *9*, 15313–15323. [CrossRef]
13. Kou, Y.; Song, X.; Guo, K.; Cheng, Z.; Wang, Y. Characterization, Thermolysis, and Energetic Properties of an MTNP/PETN Eutectic Prepared via the Solvent/Anti-Solvent Method. *Propellants Explos. Pyrotech.* **2021**, *46*, 299–308. [CrossRef]
14. Singh, J.; Staples, R.J.; Jean'ne, M.S. Coordination-driven safer and sustainable energetic materials. *J. Mater. Chem. A* **2025**, *13*, 11475–11485. [CrossRef]
15. Chen, Q.; Wu, J.; Ou, X.; Huang, B.; Almutlaq, J.; Zhumekenov, A.A.; Guan, X.; Han, S.; Liang, L.; Yi, Z. All-inorganic perovskite nanocrystal scintillators. *Nature* **2018**, *561*, 88–93. [CrossRef] [PubMed]
16. Zhang, W.-X.; Chen, S.-L.; Shang, Y.; Yu, Z.-H.; Chen, X.-M. Molecular perovskites as a new platform for designing advanced multi-component energetic crystals. *Energet. Mater. Front.* **2020**, *1*, 123–135. [CrossRef]
17. Chen, S.-L.; Yang, Z.-R.; Wang, B.-J.; Shang, Y.; Sun, L.-Y.; He, C.-T.; Zhou, H.-L.; Zhang, W.-X.; Chen, X.-M. Molecular perovskite high-energetic materials. *Sci. China Mater.* **2018**, *61*, 1123–1128. [CrossRef]
18. Feng, Y.; Zhang, J.; Cao, W.; Zhang, J.; Shreeve, J.N.M. A promising perovskite primary explosive. *Nat. Commun.* **2023**, *14*, 7765. [CrossRef]
19. Chen, S.-l.; Shang, Y.; Jiang, J.; Huang, M.; Ren, J.-T.; Guo, T.; Yu, C.-X.; Zhang, W.-X.; Chen, X.-M. A new nitrate-based energetic molecular perovskite as a modern edition of black powder. *Energet. Mater. Front.* **2022**, *3*, 122–127. [CrossRef]
20. Jia, Q.; Bai, X.; Zhu, S.; Cao, X.; Deng, P.; Hu, L. Fabrication and characterization of nano $(H_2dabco)[K(ClO_4)_3]$ molecular perovskite by ball milling. *J. Energet. Mater.* **2020**, *38*, 377–385. [CrossRef]
21. Jia, Q.; Deng, P.; Li, X.; Hu, L.; Cao, X. Insight into the thermal decomposition properties of potassium perchlorate ($KClO_4$)-based molecular perovskite. *Vacuum* **2020**, *175*, 109257. [CrossRef]
22. Deng, P.; Wang, H.; Yang, X.; Ren, H.; Jiao, Q. Thermal decomposition and combustion performance of high-energy ammonium perchlorate-based molecular perovskite. *J. Alloys Compd.* **2020**, *827*, 154257. [CrossRef]

23. Gao, Y.; Shi, E.; Deng, S.; Shiring, S.B.; Snaider, J.M.; Liang, C.; Yuan, B.; Song, R.; Janke, S.M.; Liebman-Peláez, A. Molecular engineering of organic-inorganic hybrid perovskites quantum wells. *Nat. Chem.* **2019**, *11*, 1151–1157. [CrossRef]
24. Liu, Y.; Hu, L.-S.; Gong, S.; Guang, C.; Li, L.; Hu, S.; Deng, P. Study of ammonium perchlorate-based molecular perovskite $(H_2DABCO)[NH_4(ClO_4)_3]$/graphene energetic composite with insensitive performance. *Cent. Eur. J. Energ. Mater.* **2020**, *17*, 451–469. [CrossRef]
25. Deng, P.; Guo, X.-Y.; Fang, H.; Liu, R.; Chen, P.-W. Combustion behavior and mechanism of molecular perovskite energetic material DAP-4-based composites with metal fuel Al. *Def. Technol.* **2023**, *27*, 53–63. [CrossRef]
26. Shang, Y.; Sun, L.-Y.; Ye, Z.-M.; Chen, S.-L.; Zhang, W.-X.; Chen, X.-M. Phase transition and thermal expansion of molecular perovskite energetic crystal $(C_6N_2H_{14})(NH_4)(ClO_4)_3$ (DAP-4). *FirePhysChem* **2022**, *2*, 221–225. [CrossRef]
27. Han, K.; Zhang, X.; Deng, P.; Jiao, Q.; Chu, E. Study of the thermal catalysis decomposition of ammonium perchlorate-based molecular perovskite with titanium carbide MXene. *Vacuum* **2020**, *180*, 109572. [CrossRef]
28. Deng, P.; Ren, H.; Jiao, Q. Enhanced the combustion performances of ammonium perchlorate-based energetic molecular perovskite using functionalized graphene. *Vacuum* **2019**, *169*, 108882. [CrossRef]
29. Chang, J.; Zhao, G.; Zhao, X.; He, C.; Pang, S.; Shreeve, J.N.M. New promises from an old friend: Iodine-rich compounds as prospective energetic biocidal agents. *Acc. Chem. Res.* **2020**, *54*, 332–343. [CrossRef]
30. Wei, L.; You, Z.; Meng, X.; Fang, Y.; Li, A.; Li, S.; Wang, K.; Li, Q. High-pressure exciton engineering in two-dimensional metal halide perovskite toward intense deep-blue emission and regulated photocurrent property. *Appl. Phys. Lett.* **2024**, *125*, 211901. [CrossRef]
31. Meng, X.; Wei, L.; Wu, M.; Li, A.; Li, L.; Wang, K.; Li, Q. Resolving multiple emissions of zero-dimensional heterometallic halide hybrid via pressure-triggered antenna effect. *Mater. Res. Lett.* **2024**, *12*, 417–424. [CrossRef]
32. Yan, T.-T.; Xu, Y.-F.; Xi, D.-Y.; Yu, Z.-Q.; Jiang, R.; Zhang, D.-D. High pressure study of hydrogen-bonded energetic material 4-nitropyrazole. *Phys. Lett. A* **2024**, *512*, 129567. [CrossRef]
33. Yan, T.-T.; Jiang, R.; Xi, D.-Y.; Ma, L.; Zhang, D.-D.; Xu, Y.-F. High-pressure behavior of hydrogen-bonded organic crystal trifluoroacetamide. *Chem. Phys. Lett.* **2024**, *850*, 141472. [CrossRef]
34. Ma, Z.; Li, Q.; Luo, J.; Li, S.; Sui, L.; Zhao, D.; Yuan, K.; Xiao, G.; Tang, J.; Quan, Z. Pressure-driven reverse intersystem crossing: New path toward bright deep-blue emission of lead-free halide double perovskites. *J. Am. Chem. Soc.* **2021**, *143*, 15176–15184. [CrossRef] [PubMed]
35. Zhao, D.; Wang, M.; Xiao, G.; Zou, B. Thinking about the development of high-pressure experimental chemistry. *J. Phys. Chem. Lett.* **2020**, *11*, 7297–7306. [CrossRef]
36. Yu, Z.-H.; Liu, D.-X.; Ling, Y.-Y.; Chen, X.-X.; Shang, Y.; Chen, S.-L.; Ye, Z.-M.; Zhang, W.-X.; Chen, X.-M. Periodate-based molecular perovskites as promising energetic biocidal agents. *Sci. China Mater.* **2023**, *66*, 1641–1648. [CrossRef]
37. Gagin, A.; Levin, I. Accounting for unknown systematic errors in Rietveld refinements: A Bayesian statistics approach. *J. Appl. Crystallogr.* **2015**, *48*, 1201–1211. [CrossRef]
38. Toby, B.H.; Von Dreele, R.B. GSAS-II: The genesis of a modern open-source all purpose crystallography software package. *J. Appl. Crystallogr.* **2013**, *46*, 544–549. [CrossRef]
39. Von Dreele, R.B. Small-angle scattering data analysis in GSAS-II. *J. Appl. Crystallogr.* **2014**, *47*, 1784–1789. [CrossRef]
40. Greene, R.G.; Luo, H.; Ruoff, A.L. High pressure study of AlP: Transformation to a metallic NiAs phase. *J. Appl. Phys.* **1994**, *76*, 7296–7299. [CrossRef]
41. Klotz, S.; Chervin, J.; Munsch, P.; Le Marchand, G. Hydrostatic limits of 11 pressure transmitting media. *J. Phys. D Appl. Phys.* **2009**, *42*, 075413. [CrossRef]
42. Ciezak, J.A.; Jenkins, T.A.; Liu, Z.; Hemley, R.J. High-pressure vibrational spectroscopy of energetic materials: Hexahydro-1,3,5-trinitro-1,3,5-triazine. *J. Phys. Chem. A* **2007**, *111*, 59–63. [CrossRef] [PubMed]

Disclaimer/Publisher's Note: The statements, opinions and data contained in all publications are solely those of the individual author(s) and contributor(s) and not of MDPI and/or the editor(s). MDPI and/or the editor(s) disclaim responsibility for any injury to people or property resulting from any ideas, methods, instructions or products referred to in the content.